Generation-recombination in disordered organic semiconductor: Application to the characterization of traps

Ndèye Saly Ndiaye, Olivier Simonetti, Thien-Phap Nguyen, Louis Giraudet

Version of Record: https://www.sciencedirect.com/science/article/pii/S1566119921002858
Manuscript_80c0838f33a3310bdb1023f26e73c9ac

Generation-recombination in disordered organic semiconductor: application to the characterization of traps

Ndèye Saly Ndiaye (1), Olivier Simonetti (1), Thien-Phap Nguyen (2), Louis Giraudet (1)

(1) LRN – EA 4682 – Université de Reims Champagne-Ardenne – Moulin de la Housse – BP1039 – 51687 Reims Cedex – France

(2) Institut des Matériaux Jean Rouxel, Université de Nantes - CNRS – 2, rue de la Houssinière – 44322 Nantes Cedex3 – France

Contact: olivier.simonetti@univ-reims.fr

Keywords

organic semiconductors; traps; DLTS; Gaussian density of states; generation recombination

Abstract

The presence of traps in organic semiconductor based electronic devices affects considerably their performances and their stability. The Shockley-Read-Hall (SRH) model is generally used to extract the trap parameters from the experimental results. In this paper, we propose to adapt the SRH formalism to disordered organic semiconductors by considering a hopping transport process and Gaussian distributions for both mobile and trapped carriers. The model is used to extract multiple trap parameters from charge based Deep Level Transient Spectroscopy (Q-DLTS) spectrum. Calculation of the charge transients are given in detail. The model predicts that the activation energy of the trap should not follow an Arrhenius plot on large temperature ranges. Also, the charge transients are no longer exponential when considering Gaussian trap distributions, enlarging the Q-DLTS peaks. The model fits the Q-DLTS spectra measured on organic diodes with a limited number of trap contributions with a good agreement. It is found

that an increase of the material rate of disorder reduces the extracted trap energy distances to the LUMO but has no influence on the extracted trap distribution widths. This work shows the importance of considering the specific properties of organic materials to study their properties and their trap distributions.

Introduction

The use of organic semiconductors (OSCs) in electronic devices is challenging. Organic photovoltaics (OPV), organic light emitting diodes (OLED) and organic thin-film transistors (OTFT) are used in applications such as solar energy, sensors and biosensors, flat panel displays and e-paper and circuits [1] [2] [3] [4] [5] [6] [7] [8]. Device performances are affected by the presence of traps in many ways. Traps can be located in the bulk of the semiconductor or at material interfaces and are believed to be responsible for several limitations such as instabilities or low conductivity, which then restrain their use in mainstream applications [9] [10] [11] [12] [13] [14] [15]. However, the trap formation and charge carrier trapping processes in OSC are not fully understood yet despite numerous investigations [9].

To study traps, the processes of emission and capture of carriers must be studied. Transient spectroscopy techniques have been reviewed recently by A. R. Peaker et al. [16]. One of the most efficient techniques is the Deep Level Transient Spectroscopy (DLTS). It was proposed for the first time in 1974 by D. V. Lang [17] and consists in studying the emission of trapped charges (after a filling phase of the traps) recorded as a capacitance transient (C-DLTS). The technique allows to determine the activation energy E_a of the traps and their capture cross section σ_{eff}^{t}. In the frame of the Shockley-Read-Hall (SRH) model developed for inorganic materials, charge transients are exponential functions of time, the activation energy can be clearly defined as the difference in energy between the trap level E_t and the closest transport energy level in the conduction or in the valence band. In this work we will establish that these statements will not hold when considering organic semiconductors.

In a first section, the SRH model will be briefly exposed and the parameters determining the charge transient properties will be introduced.

In a second section, we consider some specific properties of disordered OSCs: a Gaussian density of states (DOS) and a hopping transport process. In OSCs, the capture probability of a charge carrier strongly depends on its mobility [18] [19]. The mobility model proposed by Oelerich et al. [20] [21] is introduced, which appears as one of the most advanced mobility model for disordered OSCs [22]. First, we consider a Gaussian DOS for mobile carriers (the LUMO DOS) and a discrete energy level for traps. This hypothesis, which does not reflect the complexity of disorder materials, is nevertheless used to illustrate the influence of the disordered material properties on the trap characterization process.

In a third section, we consider a Gaussian DOS for both mobile and trapped carriers and study the influence of the distribution of trapped charges on the determination of the trap parameters. The choice of a Gaussian DOS for both mobile and trapped charge carriers is driven by previous studies [14] [23] [24]. In this section, we show that the charge transient does not remain exponential, broadening the DLTS peaks and modifying the trap parameter extraction process. Furthermore, we show that the activation energy of a trap cannot be strictly defined due to the complex temperature dependence of the emission frequency, and that an Arrhenius plot would not be appropriate when considering extended experimental temperature ranges. Finally, trap parameters of experimental Q-DLTS spectra [25] [26] are extracted and discussed.

Characterization of trap capture and emission: the SRH model and the DLTS method

To describe the emission and capture processes, the SRH model was proposed in 1952 to study silicon generation-recombination in silicon-based devices [27]. This formalism is often used to characterize traps in inorganic semiconductors but also in OSCs [25] [28] [29] [30] [31]. In this study, we consider only one type of mobile charge carriers (electrons). The processes of capture and emission of charge carriers is shown for electrons in Fig. 1. In this figure, e_n is the emission

frequency (in Hz) of an electron from the trap energy level E_t to the LUMO band, c_n is the capture frequency (in Hz) of a mobile electron by a trap site. n and n_t are respectively the density of mobile and trapped charge carriers. N_t is the total density of trap sites.

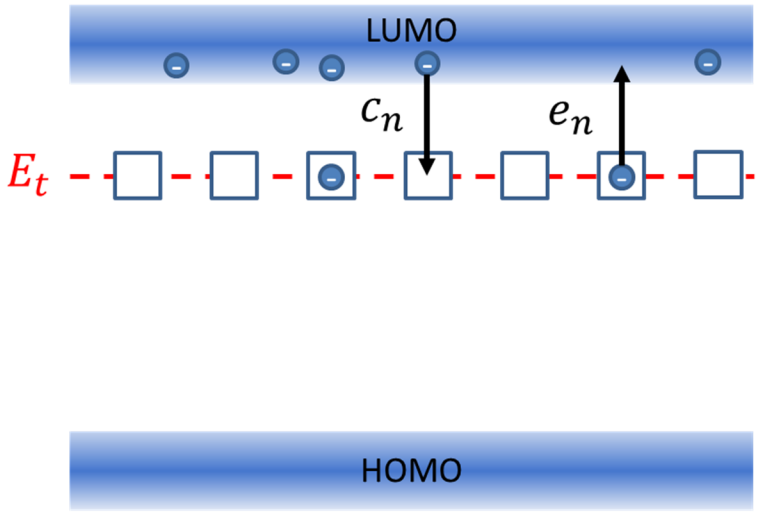

Fig. 1 Schematic representation of emission and capture processes of electrons from one discrete energy level.

To characterize a trap level E_t, one needs to calculate the emission and capture frequencies.

The emission and capture rates, respectively U_{en} and U_{cn} (expressed in $s^{-1}.cm^{-3}$), are given by Eq. 1 and Eq. 2:

Eq. 1 $$U_{en} = e_n n_t,$$

Eq. 2 $$U_{cn} = c_n n.$$

The capture frequency c_n can be expressed as (Eq. 3):

Eq. 3 $$c_n = K_t(N_t - n_t).$$

The parameter K_t depends on the capture process and the type of semiconductor, as discussed later. At thermal equilibrium, in a steady state, the number of electrons emitted from a given trap level is equal to the number of electrons captured by that trap:

Eq. 4 $U_{en} = U_{cn}$.

According to Eq. 4, it is then possible to express the emission frequency e_n as follows:

Eq. 5 $e_n = \frac{n}{n_t} c_n$.

The concentration of mobile charge carriers is given by:

Eq. 6 $n = \int_{conduction\ band} DOS(E) f(E) dE$,

where $DOS(E)$ is the density of states of mobile charge carriers and $f(E) = \frac{1}{1+\exp\left(\frac{E-E_F}{kT}\right)}$ is the Fermi-Dirac distribution for electrons, E_F is the Fermi energy level, k is the Boltzmann constant and T is the absolute temperature.

In the case of a discrete trap energy level n_t is given by:

Eq. 7 $n_t = \frac{N_t}{1+\exp\left(\frac{E_t-E_F}{kT}\right)}$.

The SRH model assumes a discrete trap level, the Boltzmann statistics $f(E) = \exp\left(-\frac{E-E_F}{kT}\right)$ and a crystalline DOS, $DOS(E) = \frac{1}{2\pi^2}\left(\frac{2m*}{\hbar^2}\right)^{\frac{3}{2}} (E - E_C)^{\frac{1}{2}}$, where m^* is the effective mass of an electron, E_C the bottom of the conduction band and ħ, the reduced Planck constant [32].

In this case, an analytical expression is obtained for the concentration of mobile charge carriers:

Eq. 8 $n = N_C \exp\left(\frac{E_F-E_C}{kT}\right)$,

where $N_C = 2\left(\frac{2\pi m^* kT}{h^2}\right)^{3/2}$ is the effective density of states of the conduction band.

In the SRH model, the parameter K_t, characteristic of the trap capture process in Eq. 3, can be expressed as:

Eq. 9 $K_t = \sigma_{eff}^t \langle v_{th} \rangle$,

where $\langle v_{th} \rangle = \sqrt{\frac{3kT}{m^*}}$ is the average thermal velocity of the mobile carriers in the conduction band, and σ_{eff}^t is the trap capture cross section. By replacing in Eq. 5 the expressions of n (Eq. 8), n_t (Eq. 7), K_t and c_n, one obtains the emission frequency (Eq. 10):

$$\text{Eq. 10} \qquad e_n = N_C \langle v_{th} \rangle \, \sigma_{eff}^t \exp\left(-\frac{(E_C - E_t)}{kT}\right).$$

Defining the trap energy activation as $E_a = (E_C - E_t)$, we can rewrite Eq. 10 as follows:

$$\text{Eq. 11} \qquad \ln\left(\frac{e_n}{T^2}\right) = -\frac{E_a}{kT} + \ln\left(\sigma_{eff}^t \Gamma_n\right),$$

where $\Gamma_n = 2\sqrt{3}\, m^* k^2 \left(\frac{2\pi}{h^2}\right)^{\frac{3}{2}}$ is a constant ($\Gamma_n = 3.26 \times 10^{25}\ \mathrm{m^{-2}s^{-1}K^{-2}}$ supposing the free electron mass for m^*).

In most trap characterization techniques, Eq. 11 is used to extract the trap parameters (i.e. E_a and σ_{eff}^t) by plotting $\ln\left(\frac{e_n}{T^2}\right) = f\left(\frac{1}{T}\right)$ for a set of temperatures, called the "Arrhenius plot". The plot is linear since the trap emission process is exponentially dependent of the activation energy: the slope of the plot actually allows for determining the activation energy E_a. The capture cross section σ_{eff}^t is extrapolated from the intersection of the Arrhenius plot with the y-axis.

In the Q-DLTS technique [17] [25] [28], during the relaxation phase of the experiment (i.e. when the trapped charges are released), providing no capture occurs thanks to an appropriate biasing sequence of the device, the emitted charge dQ_t during a time interval dt can be expressed as $dQ_t = -e_n Q_t(t) dt$, where $Q_t(t)$ is the remaining trapped charge. For a given temperature, the emission frequency e_n (Eq. 10) does not depend on the concentration of trapped carriers and is constant with time. Consequently, the previous equation can be integrated and the relaxation of the trapped charges $Q_t(t)$ follows an exponential evolution with time t as given in Eq. 12:

$$\text{Eq. 12} \qquad Q_t(t) = Q_{t0} \exp(-e_n t),$$

where Q_{t0} is the initial trapped charge, for a given temperature and biasing sequence. In practice, at a given temperature, the Q-DLTS spectrum ΔQ is plotted. $\Delta Q = Q_t(t_1) - Q_t(t_2)$ is the charge released during the time interval $[t_1, t_2]$. This technique is relevant in that it transforms an exponential transient into a response peak. For this, a new variable, call the time-window, is defined by: $\tau = \frac{t_2 - t_1}{\ln\left(\frac{t_2}{t_1}\right)}$. Usually, one takes $t_2 = 2t_1$ giving $\tau = \frac{t_1}{\ln(2)}$. Then ΔQ takes the form:

Eq. 13 $$\Delta Q(\tau) = Q_{t0} exp(-e_n \ln 2\, \tau)[1 - exp(-e_n \ln 2\, \tau)],$$

which reaches its maximum ($\Delta Q_{max} = Q_{t0}/4$) for $\tau = 1/e_n$ [25]. The trap density N_t is given by:

Eq. 14 $$N_t = \frac{Q_{t0}}{eAd},$$

where e is the electronic charge, A is the active area of the device, and d is the sample thickness.

In summary, the measurement of the charge transient and the plot of $\Delta Q(\tau)$ gives the emission rate e_n from the position of the peak maximum, at a given temperature [see Fig. 9 for an illustration of a simulated Q-DLTS peak]. Repeated experiments at various temperatures give the Arrhenius plot and finally the trap parameters (E_a, σ_{eff}^t) (see Fig. 4 for an example). Of course, in real devices trap energy levels are not discrete and one obtains multiple maxima and complex spectra, depending also on the bias sequence. However, this method appears to be relevant for the study of defects in inorganic semiconductors and has been successfully used in organic devices.

The assumptions of the SRH model are well adapted for crystalline inorganic semiconductors but should be discussed when applied to OSCs.

Adaptation of the model to organic semiconductors having a discrete trap level

To characterize traps in OSCs, the classical SRH formalism must be adapted due to the specific trap density of states of disordered organic semiconductors , and to the specific charge carrier transport mechanisms [21] [33] [34]. Gaussian and exponential trap distributions are commonly

used to characterize traps in organic semiconductors [35] [36] [37] [38] [39] [40]. The energetic distribution of mobile carriers is not determined generally but it is commonly considered to be a Gaussian [41] [33] or exponential [42] [43]. In this work a Gaussian DOS was considered, based on the work of Baranovskii [44] [24], stating that the Gaussian distribution is the one which makes it possible to explain the evolution of the mobility with the density of charge carriers.

In this part, we first considered a Gaussian DOS for the mobile carriers and discrete trap levels to study the charge trapping dynamics and the resulting characterization of traps using Q-DLTS spectra. Gaussian DOS for both mobile and trapped carriers will be treated after.

In the SRH model, the capture frequency is expressed as (Eq. 3) $c_n = K_t(N_t - n_t)$ with K_t is given by Eq. 9. Mobile charges are assumed to be delocalized and at thermal equilibrium in the conduction band. As discussed by Kuik *et al.* [18], this assumption cannot stand for semiconductors with a low carrier mobility, due to their hopping transport: considering delocalized charge carriers with a thermal velocity expressed by $\langle v_{th} \rangle = \sqrt{\frac{3kT}{m^*}}$ does not make sense in this case. To adapt the SRH model, Kuik *et al.* [18] compared the trap-assisted recombination to a biomolecular Langevin recombination [19]. This recombination process can be described as the drift of the charge carrier towards a trap (with opposite charge) driven by the Coulomb force. To avoid capture, the thermal energy of the charge carrier must be high enough to overcome the Coulombic attraction produced by the trap [19]. Following their assumption, and considering a single trap contribution, the parameter K_t in Eq. 3 becomes $K_t = \frac{e}{\varepsilon}\mu$, where μ is the mobility of charge carriers, e and ε are the elementary charge and the dielectric constant of the OSC respectively. To extend the approach of Kuik *et al.* to systems with multiple trap contributions, one must discuss the expression of the parameter K_t, since the proposed expression of the capture frequency does not depend on any of the given trap physical properties. It seems unrealistic that traps originating from various physical or chemical surroundings, would all show a single capture frequency. Consequently, we state that a K_t

parameter should be defined for each trap contribution. We then introduce the dimensionless parameter C_t related to a given trap contribution in the K_t parameter expression:

$$\text{Eq. 15} \qquad K_t = C_t \frac{e}{\varepsilon} \mu.$$

The capture frequency (Eq. 3) of a trap contribution becomes:

$$\text{Eq. 16} \qquad c_n = C_t \frac{e}{\varepsilon} \mu (N_t - n_t).$$

In most OSCs, the mobility is low because of the molecular disorder. The transport of charge carriers occurs via localized states and is described as a hopping process. The mobility then depends on the temperature, the charge carrier concentration, the shape of the DOS and the electric field [21] [22] [34] [44] [45]. Many approaches have been developed to describe the charge carrier transport in OSCs with Gaussian DOS [22]. In this study, we have used the advanced mobility model of Oelerich *et al.* [20] [21]. The model is based on the transport energy concept and considers the percolation nature of the hopping transport. The mobility model is carrier concentration dependent and is valid only at low electric field. It is well adapted to the disordered organic semiconductors under consideration. Following Oelerich *et al.* [20] the expression of the mobility is given by:

$$\text{Eq. 17} \qquad \mu \approx \nu_0 \frac{e}{kT} \frac{3 B_C F_{ER}}{4\pi\, r(E_\mu) n_{tLUMO}} \times \exp\left(-\frac{2 B_C^{1/3}}{\alpha} r(E_\mu) - \frac{E_\mu - E_F}{kT} \right)$$

where ν_0 is the attempt-to-escape frequency of the hopping process, and taken equal to $\nu_0 = 10^{12}$ Hz, $\alpha = 0.215 N_{LUMO}^{-1/3}$ is the localization length of the charge carriers and $B_C = 2.735$ is related to the percolation nature of the hopping transport [24]. N_{LUMO} is the concentration of the localized states, typically between 10^{20} cm^{-3} and 10^{21} cm^{-3}. Interested readers should refer to [21] for the concept of transport energy E_μ and the expression of the distance between localized states with energies below E_μ, $r(E_\mu)$, and refer to [46] for F_{ER} which is related to the generalized Einstein relation. Some parameters of the Gaussian disorder model depend on the actual OSC considered [47]. In the present work, due to the lack of data regarding the DOS width, the value

of the attempt-to-escape frequency, or the localization length, typical values are considered. In the transport energy concept, the charge carriers occupying energy levels above E_μ are mobile. Below this energy, carriers do not move efficiently and are considered as trapped. The concentration of the trapped charge carriers in the LUMO band is then given by $n_{tLUMO} = \int_{-\infty}^{E_\mu} DOS(E)f(E)dE$, and the concentration of mobile charge carriers in the LUMO n_{mLUMO} is given by:

$$\text{Eq. 18} \qquad n_{mLUMO} = \int_{E_\mu}^{+\infty} DOS(E)f(E)dE.$$

In the framework of the transport energy level, E_μ, the activation energy, E_a, of a trap energy level, E_t, can be defined as:

$$\text{Eq. 19} \qquad E_a = E_\mu - E_t.$$

As the transport energy E_μ depends on temperature [21], the activation energy E_a depends on temperature as well. Consequently, a single trap level E_t cannot be associated with a discrete activation energy E_a as assumed in the SRH model (Eq. 10 and Eq. 11). To the best of our knowledge, this feature has never been reported before.

Let us first consider a Gaussian DOS within the LUMO and several discrete traps. The density of mobile carriers is given by Eq. 18 with $DOS(E) = \frac{N_{LUMO}}{\sigma_{LUMO}\sqrt{2\pi}} \exp\left[-\frac{(E-E_{LUMO})^2}{2\sigma_{LUMO}^2}\right]$, where σ_{LUMO} is the width of the Gaussian, indicative of the degree of disorder in the OSC. The higher the material disorder, the larger the LUMO width (σ_{LUMO}) . A representation of the DOS is given in Fig. 2 with only one trap.

Replacing in Eq. 5 the expressions of n_{mLUMO} from Eq. 18, n_t from Eq. 7 and c_n from Eq. 16, one obtains the expression of the emission frequency:

$$\text{Eq. 20} \qquad e_n = n_{mLUMO} C_t \frac{e}{\varepsilon} \mu \left[1 + \exp\left(\frac{E_t - E_F}{kT}\right)\right].$$

For a given temperature, the emission frequency is constant with time; we still have an exponential decay of the trapped charges as in Eq. 12. Consequently, the shape of the Q-DLTS peaks will remain unchanged compared to that proposed by the SRH approach.

Calculating $\ln\left(\frac{e_n}{T^2}\right)$ from Eq. 20 will not result in a linear dependence with $\left(\frac{1}{T}\right)$ as with the SRH approach given by Eq. 11, and therefore, an Arrhenius plot would not be correctly obtained. Consequently, it is not possible to extract the trap parameters by a simple linear regression as in the classical method. In this work an optimization technique was used to extract the trap parameters from the Q-DLTS spectra.

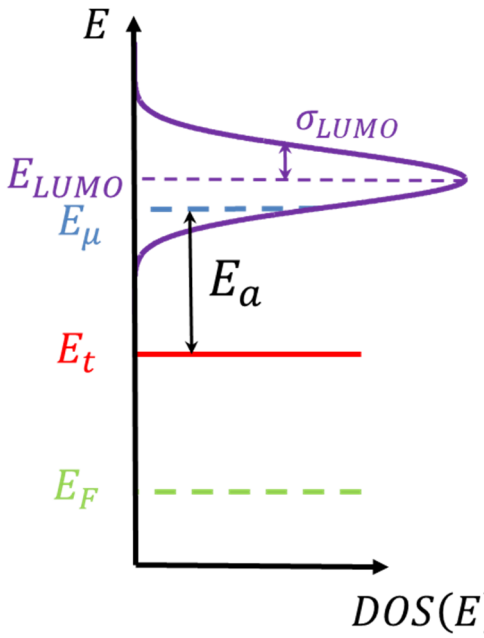

Fig. 2 Representation of the Gaussian DOS for the mobile carriers (here electrons), figuring the transport energy level E_μ, a discrete trap level E_t, and the Fermi energy level E_F during the relaxation of traps.

To validate our model, we used Q-DLTS measurements performed on an ITO/PEDOT/(PF-N-PH)/Al diode (published elsewhere [25]) in which five discrete trap levels labelled A, B, C, D and E have been identified. Fig. 3 shows the Q-DTLTS spectra used in this work, for various charging

times tc. A long charging time increases the amount of trapped charges, however not all the trap levels can be entirely filled. To take into account this feature, in the model the initial trapped charge Q_{t0} in each trap contribution is taken as a fit parameter. The charging time was fixed to 1 ms for the Q-DLTS data analysed in this work.

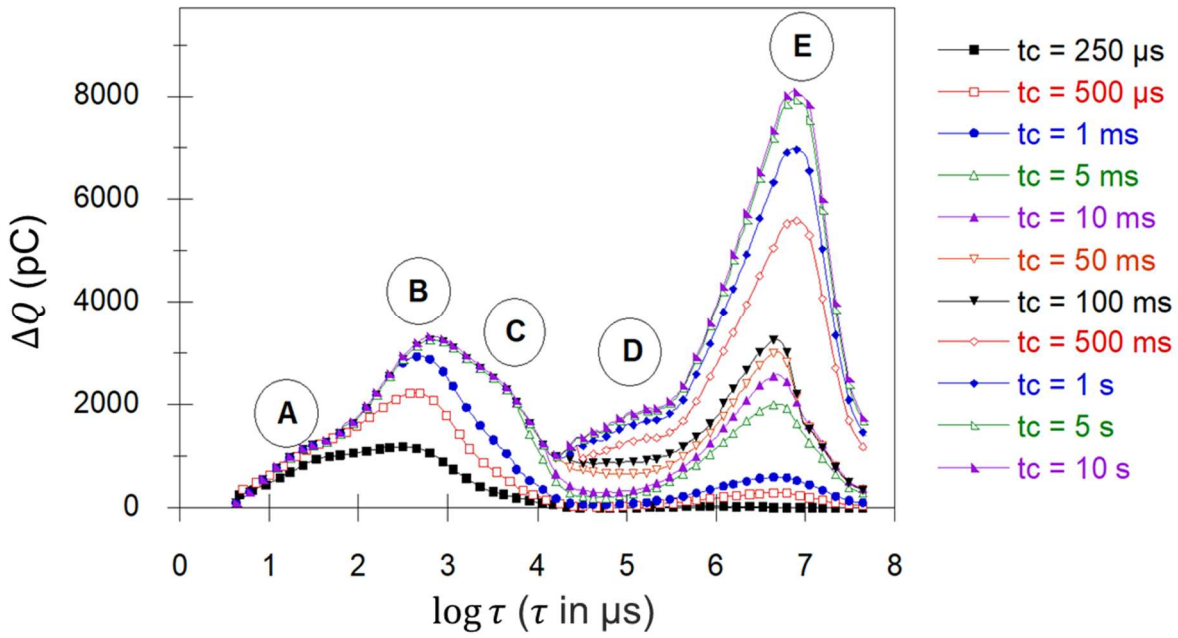

Fig. 3 Q-DLTS spectra in an ITO/PEDOT/(PF-N-PH)/Al diode for different charging times tc at $T = 300$ K [25].

Using the model given Eq. 20, we fitted the evolution of the emission frequency e_n as a function of the temperature. Fixed parameters are listed Tab. 1. Fig. 4 represents the results. For N_{LUMO}, we took the typical value for organic semiconductors. For the choice of σ_{LUMO}, we used typical values in disordered organic semiconductors. E_F was set to allow the relaxation of initially trapped charges. Simulations were performed for various Fermi level positions during the relaxation phase ($E_{LUMO} - E_F$ was varied from -0.5 to -1.5 eV), with the deepest trap level at -0.58 eV. The results showed that the Fermi level E_F does not influence the relaxation phase as long as E_F is below the deepest trap level. We took $E_{LUMO} - E_F = -1.5$ eV for all simulations.

Parameters	Values
σ_{LUMO} (meV)	80
N_{LUMO} (cm^{-3})	10^{20}
$E_{LUMO} - E_F$ (eV)	-1.5

Tab. 1 Parameters for the optimization.

In the limited temperature range of the experiment [250-310 K], the plots of $\ln\left(\frac{e_n}{T^2}\right)$ vs $\left(\frac{1}{T}\right)$, as shown Fig. 4, appear almost linear, however fitted with the non-linear expression given Eq. 20. In other words, the plots of $\ln\left(\frac{e_n}{T^2}\right)$ vs $\left(\frac{1}{T}\right)$ is non-linear but this non-linearity is not visible for a reduced range of temperatures.

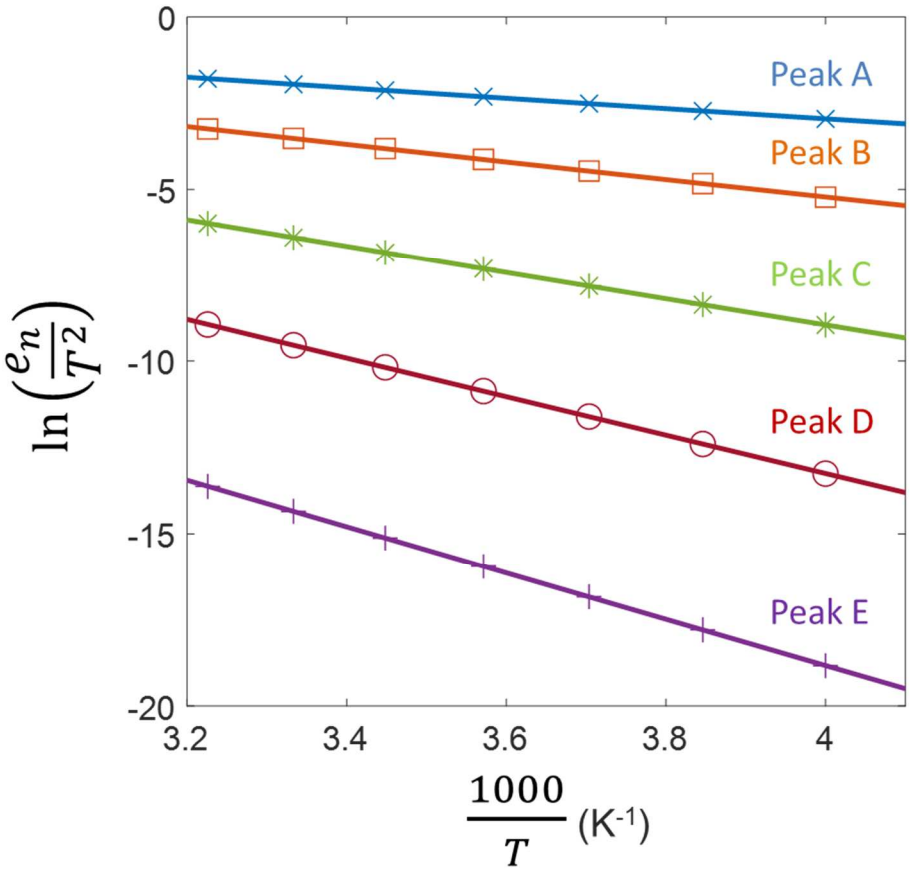

Fig. 4 Fit of the "Arrhenius plots" from [25] using our model.

To highlight the influence of the LUMO DOS on the trap parameters determined by the experiment using our model, the extracted results were compared to those of reference [25] based on usual SRH. The trap activation energies shown Fig. 5 have been extracted for $\sigma_{LUMO} =$ 80 meV. Fig. 5 a) gives the evolution of the extracted activation energies $E_a = E_\mu - E_t$ (Eq. 19) with T. One can see that the variation of E_a with T is limited because the variation of E_μ is limited due to the experimental temperature range, as shown Fig. 5 b). In the following, for the sake of clarity, we abandon the concept of activation energy, and we present only the results in terms of trap energies E_t.

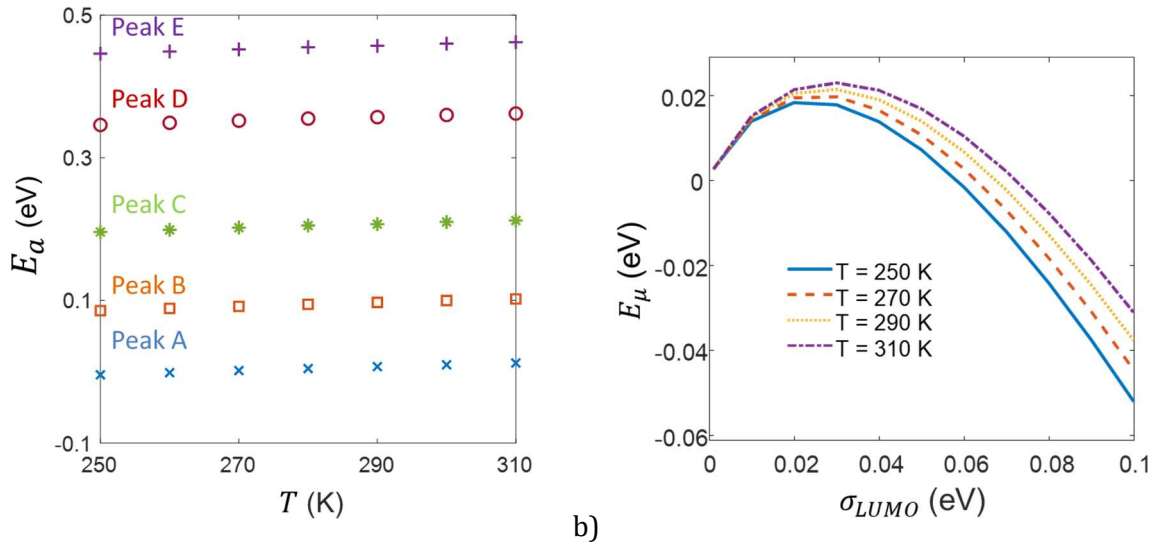

a) b)

Fig. 5 a) Evolution of the extracted activation energies with the temperature for each trap contribution. b) Evolution of the transport energy E_μ with temperature for low carrier concentration and the mean E_μ with σ_{LUMO} in the inset.

The trap parameters extracted for each trap level (see reference [25] for details) using the SRH model are given in Fig. 6 (dashed constant lines) as well as those extracted with our model for various LUMO Gaussian widths. As can be observed Fig. 6, the model predicts that the trap energy levels $E_t$depend on the degree of disorder of the material. The trap energy levels E_t are

closer to the transport band when the degree of disorder is high, i.e., when σ_{LUMO} is high. In practice, the dependence of the extracted trap energy on the transport band width is a difficulty since the Gaussian width of disordered materials is generally unknown. Also, it should be noted that by following this model, obtaining an Arrhenius trace is rather unexpected in organic devices when the experiment covers a wide temperature range. To conclude this section, considering the strong dependence of the extracted trap energies on the material DOS width, it appears mandatory to consider an appropriate model to characterize traps in organic semiconductor devices.

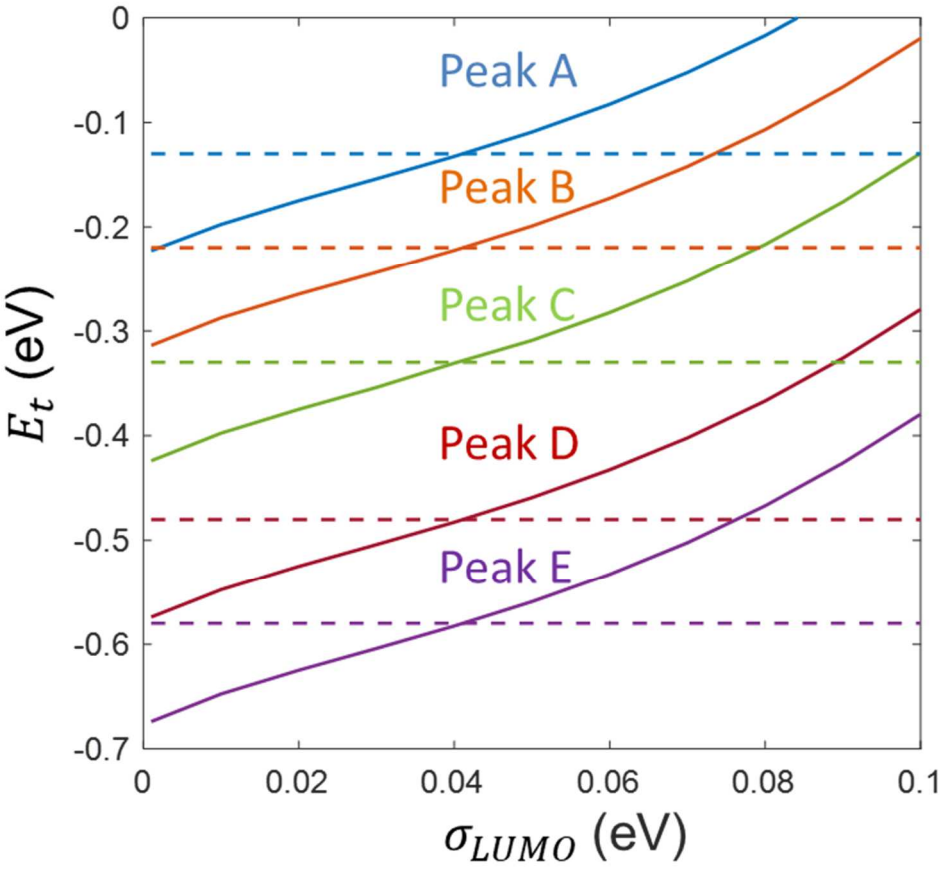

Fig. 6 Comparison between the activation energies extracted from [25] using the classical SRH method and the average activation energies extracted with our model at 300 K for different Gaussian widths.

Capture and emission processes in organic semiconductors with trap Gaussian DOS

It is unlikely that a trap level could be discrete and well defined in a disordered energetic landscape. Traps are then likely to be distributed in energy in disordered OSCs [10] [48] [49] [50]. To be more relevant we now consider Gaussian distributions for both the mobile and the trapped charges, as illustrated Fig. 7.

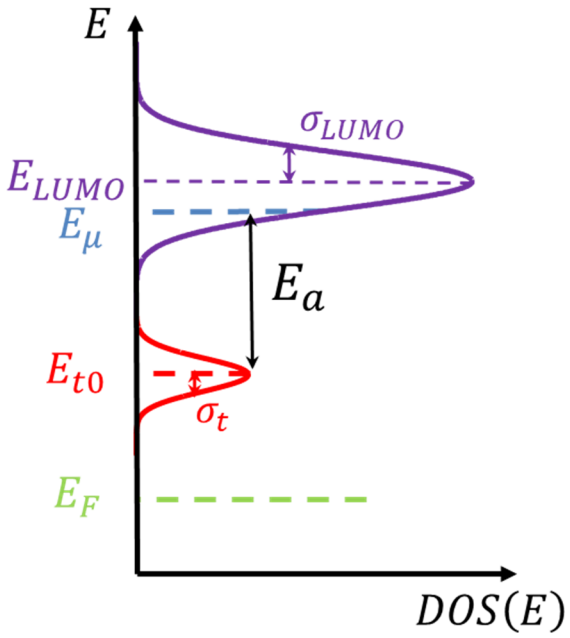

Fig. 7 Schematic of the energy distributions for electrons in OSC: a Gaussian DOS for the mobile electrons, a Gaussian distribution for the trapped electrons. The position of the Fermi level is the one that corresponds to the trap relaxation phase.

Due to the Gaussian distribution of the trapped charges, the expression of the emission frequency of the trap distribution is no longer given by Eq. 20. To calculate the emission frequency, our approach is to consider the trap Gaussian distribution as a "quasi-continuum" of discrete traps $\{E_{tj}\}$ (Fig. 8).

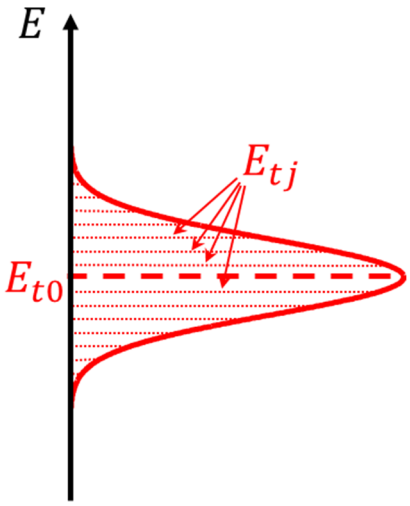

Fig. 8 A discretized Gaussian trap distribution.

The index j represents the j^{th} "discrete trap". Let we define $Q_0(E_{tj})$ as the initial amount of trapped charged at each E_{tj} during the filling stage, it is given by:

$$\text{Eq. 21} \qquad Q_0(E_{tj}) = \frac{Q_{t0}}{\sigma_t\sqrt{2\pi}} \exp\left(-\frac{(E_{tj}-E_{t0})^2}{2{\sigma_t}^2}\right) f(E_{tj})$$

where Q_{t0}, σ_t and E_{t0} are defined for a particular trap distribution and are respectively the initial trapped charge during the filling phase, the width of the trap distribution, and the distribution central energy (see Fig. 8). $f(E_{tj}) = \frac{1}{1+\exp\left(\frac{E_{tj}-E_{Ffp}}{kT}\right)}$ is the Fermi-Dirac distribution for the electrons, where E_{Ffp} is the Fermi level position during the filling phase. The amount of initially trapped charges given in Eq. 21 depends on the capture probability of mobile carriers c_n which is constant for a given temperature. We suppose that the Fermi level was set appropriately during the filling phase, i.e., above all the trap sites to ensure efficient capture. Within a Gaussian distribution the discrete trap sites will be considered to have the same probability to capture a mobile carrier, which is equivalent to consider that $f(E_{tj}) \approx 1$. In other words, the trap Gaussian distribution is considered as uniformly occupied after the filling phase.

During the relaxation phase, each "discrete trap" level, E_{tj}, can release $Q(E_{tj}, t)$ charges following:

Eq. 22 $$Q(E_{tj}, t) = Q_0(E_{tj}) \exp(-e_n(E_{tj}).t),$$

where $e_n(E_{tj})$ is the emission frequency of an electron from the "discrete trap" level E_{tj} to the LUMO and is given by Eq. 20 with E_t replaced by E_{tj}:

Eq. 23 $$e_n(E_{tj}) = n_{mLUMO} C_t \frac{e}{\varepsilon} \mu \left[1 + \exp\left(\frac{E_{tj} - E_F}{kT}\right)\right].$$

Finally, considering Eq. 21 and Eq. 22 with $f(E_{tj}) \approx 1$ the total released trapped charges of a particular trap contribution is given by:

Eq. 24 $$Q(t) = \int_{-\infty}^{+\infty} \frac{Q_{t0}}{\sigma_t \sqrt{2\pi}} \exp\left(-\frac{(E_{tj} - E_{t0})^2}{2{\sigma_t}^2}\right) \exp(-e_n(E_{tj}).t)\, dE_{tj}.$$

A Gaussian trap contribution is then characterized by three parameters: the Gaussian width of the trap distribution, σ_t, the maximum of the trap distribution, E_{t0}, and the dimensionless parameter C_t introduced in Eq. 15.

In order to test the model represented by Eq. 24, we use previously published experimental Q-DLTS spectra [26] (Fig. 10). The experimental Q-DLTS spectra used in this study were recorded from a perovskite based N-I-P solar cell structure from 250 to 320 K [26]. The SRH model was used to extract six discrete trap contributions in PBTTTV-h (see the Table 4 in the reference [26]). The PBTTTV-h is a thiophene-based two-dimensional conjugated polymer of poly{3-(5,5"-di(2-ethylhexyl)-2,2':5',2"-terthienyl-3'-vinyl)-thio-phene-alt-thiophene} (insert in Fig. 10).

Our approach consisted in calculating the Q-DLTS spectrum for a number of Gaussian trap contributions using Eq. 24, to fit the data. A standard non-linear optimization technique was used to extract the trap parameters.

The following list details the fitted parameters and their initial values:

- As can be seen in Fig. 10, the amplitudes of the various Q-DLTS peaks, corresponding to the various trap distributions, vary with temperature. This is partly due to variations of the initial amount of trap charges Q_{t0} over the various trap distributions after the filling phase. This charge Q_{t0} depends both on temperature, filling time (see Fig. 3), and generally on the sample biasing history. Despite the filling phase being set so as to minimize these fluctuations, some variations remain. Therefore, the amount of initial trapped charges in each trap distribution and at each temperature (Q_{t0}) were fitted parameters. Initial values were set by manual adjustment to obtain an initial approximate agreement.
- The central energy of each trap distribution E_{t0} is a fitting parameter. Initial values were set based on the activation energies obtained in [26].
- The dimensionless parameter C_t introduced in Eq. 15 is a fitting parameter. Initial values are also chosen based on reference [26]. With Eq. 9 and Eq. 15 the initial guess C_{t0} is calculated with the formula: $C_{t0} = \frac{\varepsilon}{\mu e}\sigma_{eff}^{t}\langle v_{th}\rangle$.
- The Gaussian width of each trap distribution σ_t was optimized as well. Initial values were taken around 100 meV. As expected, the trap distribution width modulates the width of the Q-DLTS peaks. This is illustrated Fig. 9 in which, Q-DLTS peaks are simulated for different Gaussian widths. The width of the Q-DLTS peak increases with the trap width σ_t. A narrow Gaussian distribution behaves as a discrete trap (dashed line in Fig. 9).

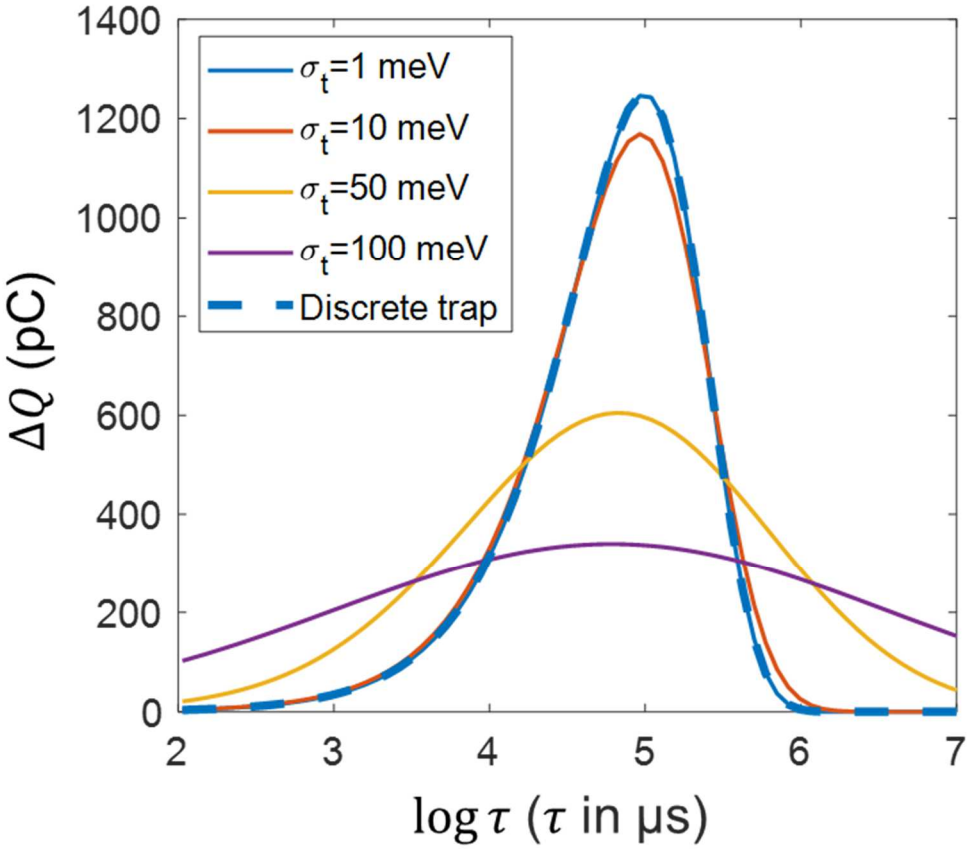

Fig. 9 Illustration of the influence of the Gaussian width σ_t of a trap distribution on the Q-DLTS peak, and comparison with a discrete trap (dashed line). Increasing the trap distribution width broadens the Q-DLTS peak.

The following parameters are also required (see Tab. 1):

- The Gaussian width of the DOS of the mobile carriers σ_{LUMO} is set to 50 meV. This value, actually unknown in the sample under study, is typical of disordered organic semiconductors [33].
- The total density of states in the LUMO N_{LUMO} is taken equal to 10^{20} cm^{-3}.
- The Fermi level $E_F - E_{LUMO}$ during the relaxation phase is set to -1.5 eV.

The results of the optimizations are given in Fig. 10 and Tab. 2. A correct fit can be obtained considering three Gaussian trap distributions instead of six in the reference [26] when using the

SRH model. This is due to the enlargement of the Q-DLTS peaks when considering trap Gaussian distributions. Several comments can be made on the results.

The trap energy levels are close to each other and very close to the LUMO. To our knowledge this behaviour is not usual. This might be because the SRH method is used in the literature to extract trap parameters [25] [51] or because a single discrete trap contribution is considered as in the technic which uses SCLC measurements [52]. In comparison with previous studies, our approach is thought to give a more realistic view of the trap behaviour in organic semiconductors.

The attempt-to-escape frequency values, $\nu_{t0} = n_{mLUMO} C_t \frac{e}{\varepsilon} \mu$, of traps can be calculated from the fitted C_t parameter. The calculated values are consistent with the range of values found in the literature [52]. However, we must emphasize that only a weak confidence can be given to these values, due to the limited experimental temperature range (here 250-320 K), since over a limited temperature range both E_{t0} and ν_{t0} have similar effect on the Q-DLTS peaks and are strongly correlated: both parameters translate the Q-DLTS spectra along the relaxation time axis. To evaluate a confidence interval, from the optimum fit, a range of values achieving an acceptable error was determined and are indicated in Tab. 2. The threshold of the relative error increase was set to 50%, with almost no observable effect (by eye) on the spectra. From Tab. 2 one can evaluate the relatively large variation range of each optimized parameter. Unfortunately, due to device stability issues, the experimental temperature range can hardly be extended and one has to rely on these confidence interval.

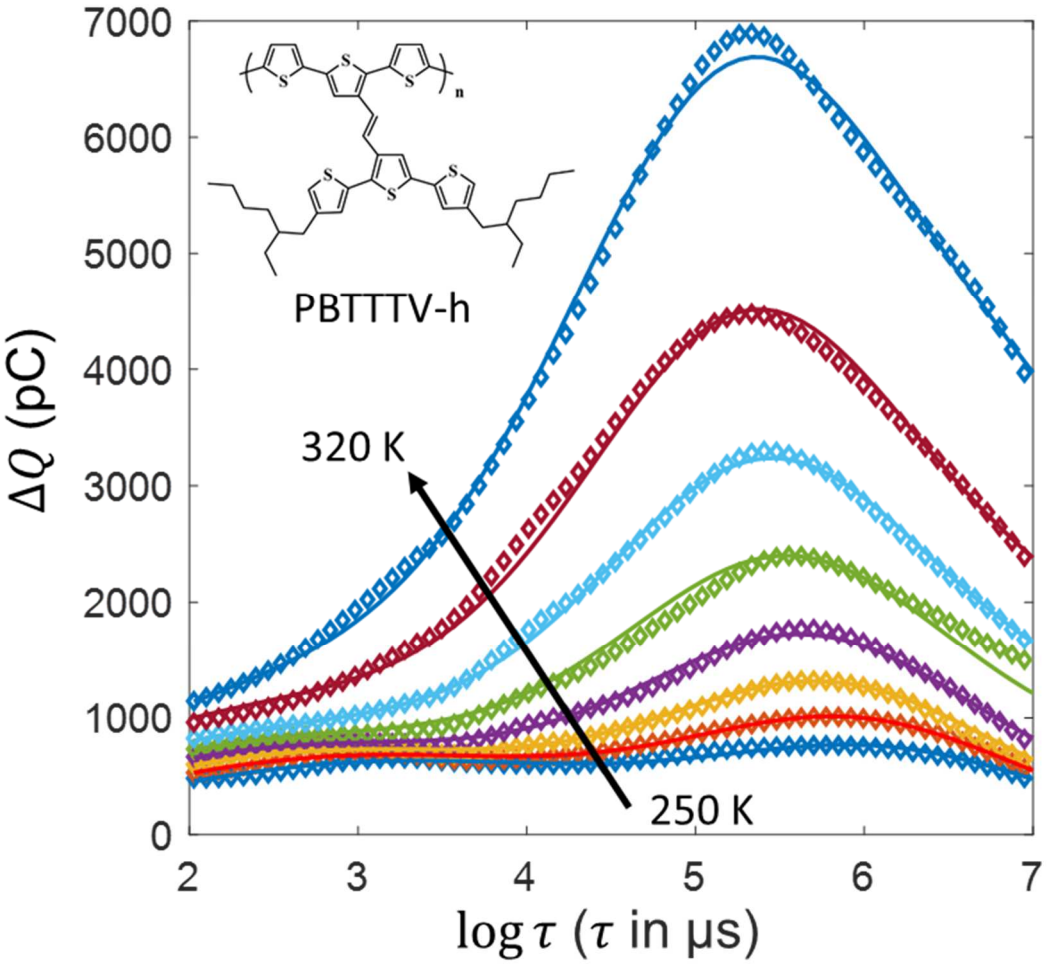

Fig. 10 Experimental (circles) from [26] and simulated Q-DLTS response (continuous lines) at different temperatures obtained with a Gaussian DOS for mobile carriers (parameters are given in Tab. 1 with $\sigma_{LUMO} = 50\,meV$) and three Gaussian trap contributions. Optimized parameters are given in Tab. 2.

Trap contributions	1	2	3
$E_{LUMO} - E_{t0}$ (eV) (optimum)	-0.160	-0.215	-0.182

$E_{LUMO} - E_{t0}$ (eV) (range)	$[-0.13, -0.185]$	$[-0.015, -0.415]$	$[-0.103, -0.283]$
C_t (optimum)	2.9×10^{-5}	2.9×10^{-5}	7.1×10^{-2}
C_t (range)	$[8.5 \times 10^{-6}, 8.8 \times 10^{-4}]$	$[1.7 \times 10^{-8}, 5.3 \times 10^{-2}]$	$[2 \times 10^{-3}, 6.3]$
σ_t (meV)	44	104	67
N_t (cm^{-3}) @ 320 K	1.9×10^{17}	7.4×10^{17}	8.1×10^{16}

Tab. 2 Result of the final optimization of the Q-DLTS measurements of Fig. 10 by fixing C_t and for $\sigma_{LUMO} = 50$ meV.

The evolution in temperature of the initially trapped charges for each trap distribution is given in Fig. 11. The amount of trapped charges Q_{t0} increases with temperature. This behaviour is coherent with the physics of the trapping processes and the mobility temperature dependence in disordered materials. The capture frequency (Eq. 16) depends on the carrier mobility following $c_n = C_t \frac{e}{\varepsilon} \mu (N_t - n_t)$. As in disordered semiconductors the transport is hopping based, the carrier mobility is activated by temperature. Therefore, the capture process is accelerated during the filling phase when increasing the temperature, increasing in turn the trapped charge density and consequently the corresponding Q-DLTS peaks. This is experimentally observed (Fig. 3 and Fig. 10).

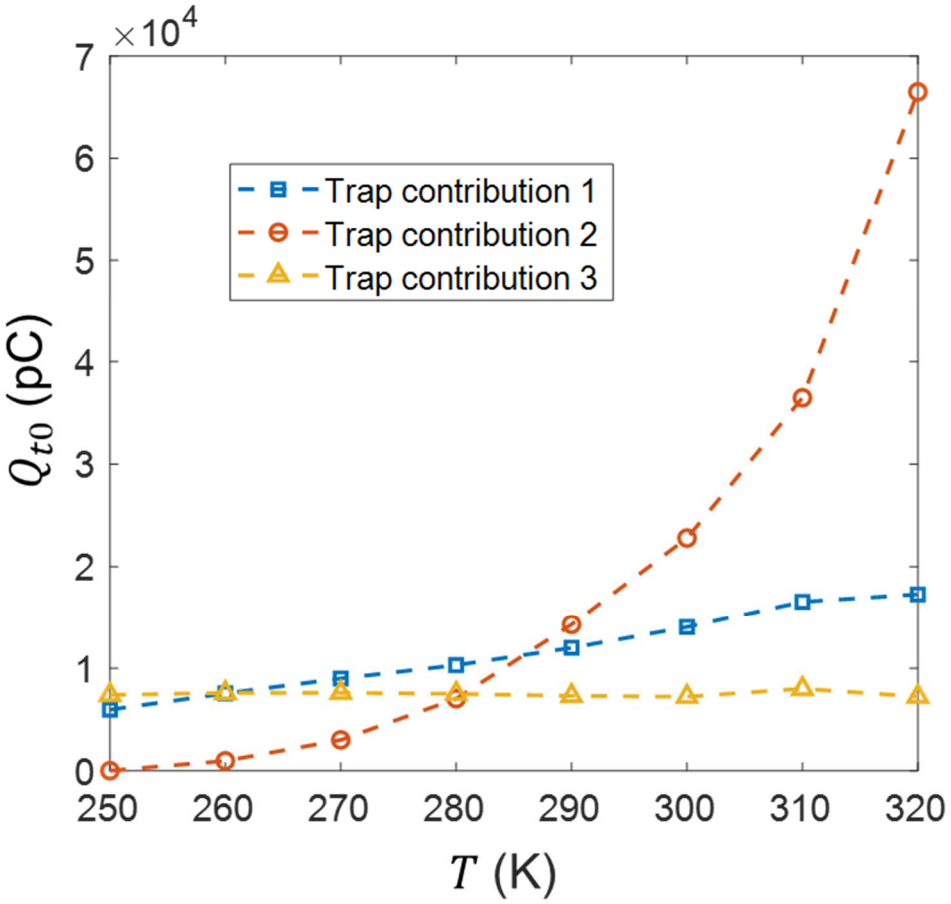

Fig. 11 Evolution of Q_{t0} of each contribution obtained after the optimization of the data with the temperature.

The energetic distribution of the three trap contributions is given Fig. 12, figuring the uncertainty intervals as described above. From these distributions, we calculated the density of trap sites N_t given in Tab. 2 using Eq. 14. The diode active area is $A = 0.07$ cm² and the semiconductor thickness is $d = 80$ nm [26]. The trap densities are in agreement with the values obtained in [26]. This agreement is obviously required since the trap densities are directly linked to the amplitude of the charge transients, these experimental facts are independent of the model used.

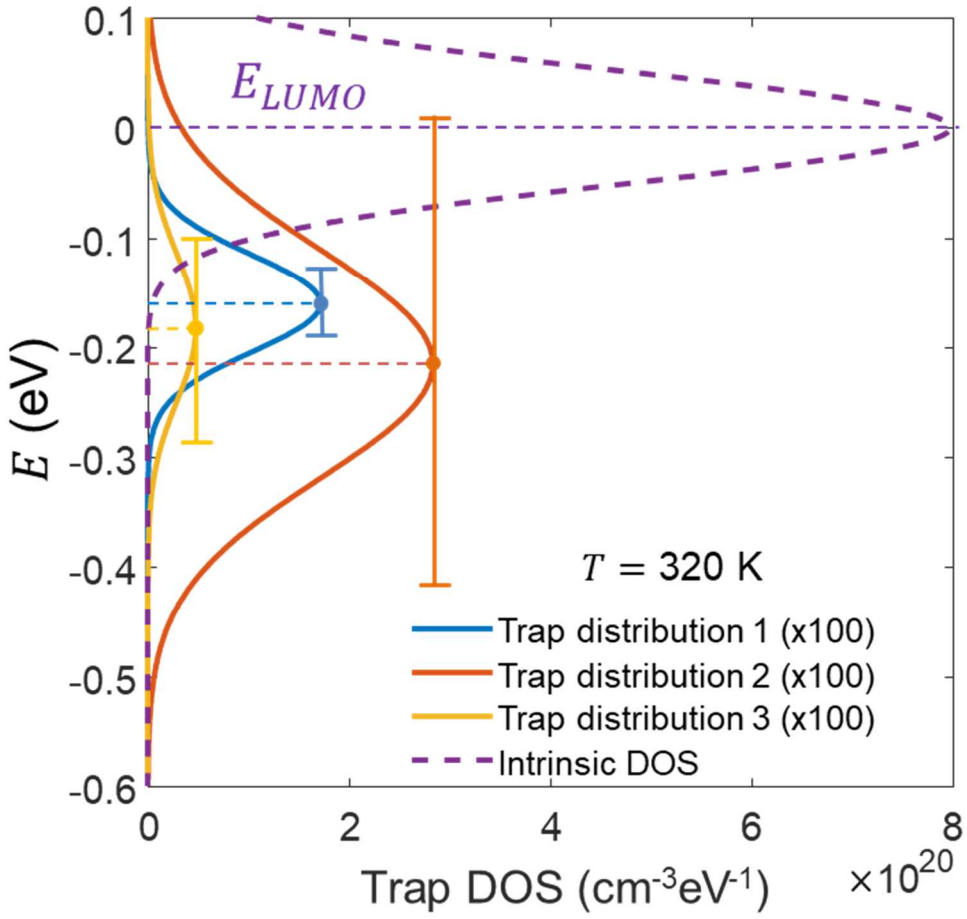

Fig. 12 Representation of the DOS of the three trap contributions at 320 K (plain lines, note the x100 magnification), and the intrinsic DOS (dashed purple line). The error bars represent the trap energy ranges giving an acceptable Q-DLTS spectrum fit (when varying only a given trap energy).

As mentioned above, the LUMO width in disordered semiconductors is difficult to evaluate and might be different from sample-to-sample and lab-to-lab due to the intrinsic nature of these disordered materials. It is unknown in the sample under study. A Gaussian width σ_{LUMO} of 50 meV was chosen in this study because this value is in the range of commonly used values. In order to evaluate the dependence of the extracted trap parameters on the intrinsic DOS width, the optimization process was repeated with LUMO DOS widths of 75 meV and 100 meV. The results are given Fig. 13. The extracted trap energies depend strongly on the width of the LUMO

DOS as previously established with discrete traps (Fig. 6). In contrast the extracted trap distribution widths remain stable when varying the LUMO DOS width.

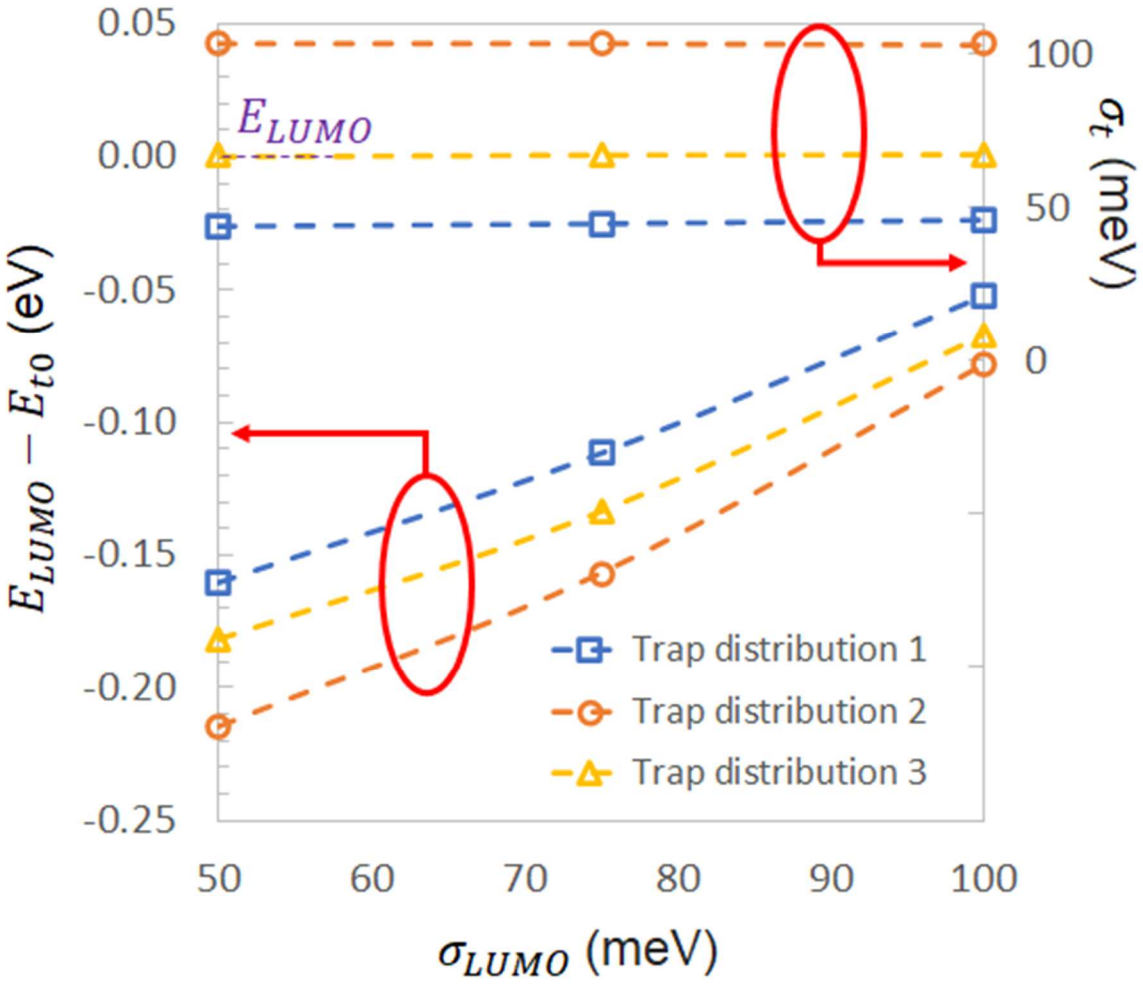

Fig. 13 Evolution of the trap parameters extracted from the Q-DLTS spectra (Fig. 10) with the intrinsic DOS width σ_{LUMO}.

The influence of the total density of states in the LUMO was also studied. The optimization process was repeated for LUMO density of states (N_{LUMO}) in the range of 5.10^{19} to 1.10^{21} cm^{-3}. It was found that the extracted trap parameters were almost insensitive to the LUMO total density of states. The three trap energies are reduced by only 20meV when increasing N_{LUMO} in this range, with no noticeable change of the three trap DOS widths.

From the various extractions, it appears that mainly the material rate of disorder, (i.e. the LUMO width), impacts directly the extracted trap energies: increasing the rate of disorder brings the extracted trap distribution closer to the LUMO. The other extracted trap parameters are mostly independent of the material intrinsic DOS. To enhance the reliability of extracted trap parameters, in particular the trap energies, it is of prime importance to the study of the density of states of organic semiconductors. Other techniques such as the fractional thermally stimulated current (TSC) [53] or the thermally stimulated luminescence (TSL) [54]. could be usefully considered to complementally probe the DOS.

We have developed a model to characterize trap parameters in organic semiconductors. The model considers the specific transport mechanisms in organic semiconductors and the Gaussian shape of the DOS for the mobile and trapped charges as well. We have accurately fitted the experimental data with a limited number of trap distributions. Limitations of the method have been studied. A larger temperature range would allow de-embedding E_{t0} and C_t (or ν_{t0}), however such experiments are not possible due to device stability issues. Also, in order to more precisely assess the trap distribution energies E_{t0}, a good knowledge of the density of states of organic semiconductors is mandatory.

Conclusion

In this study, a model for the characterization of traps in disordered organic semiconductors has been adapted from the conventional Shockley-Read-Hall formalism and from previous developments for organic low mobility materials. The model considers the main specificities of disordered OSCs: Gaussian density of states and hopping transport. The charge transport model considered is the mobility model developed by Oelerich *et al.* The model is applied to the analysis of previously published measurements using the Q-DLTS technique.

We have highlighted the importance of considering the shape of the density of states for both mobile and trapped carriers instead of the SRH model established for inorganic semiconductors.

A first model has been derived considering the LUMO Gaussian DOS and discrete trap energies, allowing a number of statements to be established. It was shown that the concept of activation energy should be discussed. Indeed, if the activation energy is defined as the difference between the transport energy and the trap level, it has been established that the activation energy of the trap should not be constant with temperature. This is due to the variation of the transport energy with temperature in disordered semiconductors. Consequently, an Arrhenius plot over an extended temperature range should not be observed in disordered semiconductors. Also, evidence was given of the dependence of the position of the traps with the LUMO Gaussian width, often unknown. This first model did not allow to reproduce the large Q-DLTS peaks experimentally observed, since for a single trap level the charge detrapping transient is still exponential at a given temperature even with a Gaussian LUMO DOS.

It appeared then necessary to develop a more advanced approach considering Gaussian DOS for both the LUMO and the trap distributions. This model is believed to better describe the trap energetic landscape in disordered semiconductors. With this advanced model, the Q-DLTS spectra could be well fitted with only three trap contributions instead of six discrete levels using the SRH approach. This could be mainly due to the broadening of the Q-DLTS peaks resulting from the energy spreading of the traps within their respective distributions.

For each trap distribution, a number of parameters were extracted. The reliability of the extracted values was discussed with respect to various unknown parameters of the sample or due to the limited temperature range of the experiment. It was shown that the LUMO width, i.e. the rate of disorder of the organic material, is the most sensitive parameter in the process of extracting trap data from Q-DLTS spectra. The width of the LUMO density of states influences the positions of the trap energy levels but not their own distribution widths. The trap distributions are found closer to the transport band when the degree of disorder is high. Finally, the extraction process revealed trap distributions close to the LUMO edge, with relatively large DOS.

Considering the high density of trap states (10^{17} cm^{-3}), should these traps be considered as tail states is an open question.

To conclude, a new model is proposed to describe defect states in disordered organic semiconductors considering a Gaussian distribution for both mobile and trapped carriers. Good agreement with experimental data is obtained by the Q-DLTS technique. Analysis of the reliability of the extracted trap parameters emphasized the need of a better knowledge of the LUMO characteristics in these materials. The present model is expected to help understanding some experimental results of disordered semiconductor materials.

Acknowledgment

This work was financially supported by the Grand-Est region and the European Community through the FEDER project POLCA. Some of the experiments were carried out within the Nanomat platform (www.nanomat.eu) supported by the Ministère de l'Enseignement Supérieur et de la Recherche, the Région Grand Est, and FEDER funds from the European Community.

References

[1] M. Moser, A. Wadsworth, N. Gasparini, and I. McCulloch, "Challenges to the Success of Commercial Organic Photovoltaic Products," *Adv. Energy Mater.*, p. 2100056, Mar. 2021, doi: 10.1002/aenm.202100056.

[2] O. Abdulrazzaq, V. Saini, S. Bourdo, E. Dervishi, and A. Biris, "Organic Solar Cells: A Review of Materials, Limitations, and Possibilities for Improvement," *Particulate Science and Technology*, vol. 31, Sep. 2013, doi: 10.1080/02726351.2013.769470.

[3] R. Ganesamoorthy, G. Sathiyan, and P. Sakthivel, "Review: Fullerene based acceptors for efficient bulk heterojunction organic solar cell applications," *Solar Energy Materials and Solar Cells*, vol. 161, pp. 102–148, Mar. 2017, doi: 10.1016/j.solmat.2016.11.024.

[4] M. Y. Lee, H. R. Lee, C. H. Park, S. G. Han, and J. H. Oh, "Organic Transistor-Based Chemical Sensors for Wearable Bioelectronics," *Acc. Chem. Res.*, vol. 51, no. 11, pp. 2829–2838, Nov. 2018, doi: 10.1021/acs.accounts.8b00465.

[5] L. Torsi, M. Magliulo, K. Manoli, and G. Palazzo, "Organic field-effect transistor sensors: a tutorial review," *Chem. Soc. Rev.*, vol. 42, no. 22, p. 8612, 2013, doi: 10.1039/c3cs60127g.

[6] Y. H. Lee, M. Jang, M. Y. Lee, O. Y. Kweon, and J. H. Oh, "Flexible Field-Effect Transistor-Type Sensors Based on Conjugated Molecules," *Chem*, vol. 3, no. 5, pp. 724–763, Nov. 2017, doi: 10.1016/j.chempr.2017.10.005.

[7] A. F. Paterson *et al.*, "Recent Progress in High-Mobility Organic Transistors: A Reality Check," *Adv. Mater.*, vol. 30, no. 36, p. 1801079, Sep. 2018, doi: 10.1002/adma.201801079.

[8] G. Gelinck, P. Heremans, K. Nomoto, and T. D. Anthopoulos, "Organic Transistors in Optical Displays and Microelectronic Applications," *Adv. Mater.*, vol. 22, no. 34, pp. 3778–3798, Sep. 2010, doi: 10.1002/adma.200903559.

[9] H. F. Haneef, A. M. Zeidell, and O. D. Jurchescu, "Charge carrier traps in organic semiconductors: a review on the underlying physics and impact on electronic devices," *J. Mater. Chem. C*, vol. 8, no. 3, pp. 759–787, Jan. 2020, doi: 10.1039/C9TC05695E.
[10] D. Abbaszadeh *et al.*, "Electron Trapping in Conjugated Polymers," *Chem. Mater.*, vol. 31, no. 17, pp. 6380–6386, Sep. 2019, doi: 10.1021/acs.chemmater.9b01211.
[11] S. Bisoyi *et al.*, "A comprehensive study of charge trapping in organic field-effect devices with promising semiconductors and different contact metals by displacement current measurements," *Semicond. Sci. Technol.*, vol. 31, no. 2, p. 025011, Feb. 2016, doi: 10.1088/0268-1242/31/2/025011.
[12] P. A. Bobbert, A. Sharma, S. G. J. Mathijssen, M. Kemerink, and D. M. de Leeuw, "Operational Stability of Organic Field-Effect Transistors," *Advanced Materials*, vol. 24, no. 9, pp. 1146–1158, 2012, doi: https://doi.org/10.1002/adma.201104580.
[13] H. Sirringhaus, "Reliability of Organic Field-Effect Transistors," *Adv. Mater.*, vol. 21, no. 38–39, pp. 3859–3873, Oct. 2009, doi: 10.1002/adma.200901136.
[14] H. T. Nicolai *et al.*, "Unification of trap-limited electron transport in semiconducting polymers," *Nature Mater*, vol. 11, no. 10, pp. 882–887, Oct. 2012, doi: 10.1038/nmat3384.
[15] G. Zuo, M. Linares, T. Upreti, and M. Kemerink, "General rule for the energy of water-induced traps in organic semiconductors," *Nat. Mater.*, vol. 18, no. 6, pp. 588–593, Jun. 2019, doi: 10.1038/s41563-019-0347-y.
[16] A. R. Peaker, V. P. Markevich, and J. Coutinho, "Tutorial: Junction spectroscopy techniques and deep-level defects in semiconductors," *Journal of Applied Physics*, vol. 123, no. 16, p. 161559, Apr. 2018, doi: 10.1063/1.5011327.
[17] D. V. Lang, "Deep-level transient spectroscopy: A new method to characterize traps in semiconductors," *Journal of Applied Physics*, vol. 45, no. 7, pp. 3023–3032, Jul. 1974, doi: 10.1063/1.1663719.
[18] M. Kuik, L. J. A. Koster, G. A. H. Wetzelaer, and P. W. M. Blom, "Trap-Assisted Recombination in Disordered Organic Semiconductors," *Phys. Rev. Lett.*, vol. 107, no. 25, p. 256805, Dec. 2011, doi: 10.1103/PhysRevLett.107.256805.
[19] M. Pope, *Electronic Processes in Organic Crystals and Polymers*, Oxford University Press USA. 1999.
[20] J. O. Oelerich, D. Huemmer, and S. D. Baranovskii, "How to Find Out the Density of States in Disordered Organic Semiconductors," *Phys. Rev. Lett.*, vol. 108, no. 22, p. 226403, May 2012, doi: 10.1103/PhysRevLett.108.226403.
[21] S. D. Baranovskii, "Mott Lecture: Description of Charge Transport in Disordered Organic Semiconductors: Analytical Theories and Computer Simulations," *Phys. Status Solidi A*, vol. 215, no. 12, p. 1700676, Jun. 2018, doi: 10.1002/pssa.201700676.
[22] O. Simonetti and L. Giraudet, "Transport models in disordered organic semiconductors and their application to the simulation of thin-film transistors," *Polymer International*, vol. 68, no. 4, pp. 620–636, 2019, doi: https://doi.org/10.1002/pi.5768.
[23] H. T. Nicolai, M. M. Mandoc, and P. W. M. Blom, "Electron traps in semiconducting polymers: Exponential versus Gaussian trap distribution," *Phys. Rev. B*, vol. 83, no. 19, p. 195204, May 2011, doi: 10.1103/PhysRevB.83.195204.
[24] A. V. Nenashev, J. O. Oelerich, and S. D. Baranovskii, "Theoretical tools for the description of charge transport in disordered organic semiconductors," *J. Phys.: Condens. Matter*, vol. 27, no. 9, p. 093201, Mar. 2015, doi: 10.1088/0953-8984/27/9/093201.
[25] T. P. Nguyen, "Defects in organic electronic devices," *phys. stat. sol. (a)*, vol. 205, no. 1, pp. 162–166, Jan. 2008, doi: 10.1002/pssa.200776805.
[26] H.-C. Hsieh *et al.*, "Analysis of Defects and Traps in N–I–P Layered-Structure of Perovskite Solar Cells by Charge-Based Deep Level Transient Spectroscopy (Q-DLTS)," *J. Phys. Chem. C*, vol. 122, no. 31, pp. 17601–17611, Aug. 2018, doi: 10.1021/acs.jpcc.8b01949.
[27] W. Shockley and W. T. Read, "Statistics of the Recombinations of Holes and Electrons," *Phys. Rev.*, vol. 87, no. 5, pp. 835–842, Sep. 1952, doi: 10.1103/PhysRev.87.835.

[28] J. A. Carr, M. Elshobaki, and S. Chaudhary, "Deep defects and the attempt to escape frequency in organic photovoltaic materials," *Appl. Phys. Lett.*, vol. 107, no. 20, p. 203302, Nov. 2015, doi: 10.1063/1.4936160.
[29] Y. S. Yang *et al.*, "Deep-level defect characteristics in pentacene organic thin films," *Appl. Phys. Lett.*, vol. 80, no. 9, pp. 1595–1597, Mar. 2002, doi: 10.1063/1.1459117.
[30] S. Neugebauer, J. Rauh, C. Deibel, and V. Dyakonov, "Investigation of electronic trap states in organic photovoltaic materials by current-based deep level transient spectroscopy," *Appl. Phys. Lett.*, vol. 100, no. 26, p. 263304, Jun. 2012, doi: 10.1063/1.4731637.
[31] L. Stuchlikova, M. Weis, P. Juhasz, A. Kosa, L. Harmatha, and J. Jakabovic, "Defect Analysis of Pentacene Diode," *Acta Physica Polonica A*, vol. 125, pp. 1038–1041, Mar. 2014, doi: 10.12693/APhysPolA.125.1038.
[32] S. M. Sze, *Physics of semiconductor devices*. New York : Wiley, 1981. Accessed: Mar. 24, 2021. [Online]. Available: http://archive.org/details/physicsofsemicon0000_2ed
[33] H. Bässler and A. Köhler, "Charge Transport in Organic Semiconductors," in *Unimolecular and Supramolecular Electronics I*, vol. 312, R. M. Metzger, Ed. Berlin, Heidelberg: Springer Berlin Heidelberg, 2011, pp. 1–65. doi: 10.1007/128_2011_218.
[34] N. Tessler, Y. Preezant, N. Rappaport, and Y. Roichman, "Charge Transport in Disordered Organic Materials and Its Relevance to Thin-Film Devices: A Tutorial Review," *Adv. Mater.*, vol. 21, no. 27, pp. 2741–2761, Jul. 2009, doi: 10.1002/adma.200803541.
[35] J. Dacuña, W. Xie, and A. Salleo, "Estimation of the spatial distribution of traps using space-charge-limited current measurements in an organic single crystal," *Phys. Rev. B*, vol. 86, no. 11, p. 115202, Sep. 2012, doi: 10.1103/PhysRevB.86.115202.
[36] J. Dacuña and A. Salleo, "Modeling space-charge-limited currents in organic semiconductors: Extracting trap density and mobility," *Phys. Rev. B*, vol. 84, no. 19, p. 195209, Nov. 2011, doi: 10.1103/PhysRevB.84.195209.
[37] V. Kumar *et al.*, "Carrier transport in conducting polymers with field dependent trap occupancy," *Journal of Applied Physics*, vol. 92, no. 12, pp. 7325–7329, Dec. 2002, doi: 10.1063/1.1523142.
[38] A. Sharma, S. Yadav, P. Kumar, S. Ray Chaudhuri, and S. Ghosh, "Defect states and their energetic position and distribution in organic molecular semiconductors," *Appl. Phys. Lett.*, vol. 102, no. 14, p. 143301, Apr. 2013, doi: 10.1063/1.4801636.
[39] R. Rohloff, N. B. Kotadiya, N. I. Crăciun, P. W. M. Blom, and G. a. H. Wetzelaer, "Electron and hole transport in the organic small molecule α-NPD," *Appl. Phys. Lett.*, vol. 110, no. 7, p. 073301, Feb. 2017, doi: 10.1063/1.4976205.
[40] A. J. Campbell, D. D. C. Bradley, and D. G. Lidzey, "Space-charge limited conduction with traps in poly(phenylene vinylene) light emitting diodes," *Journal of Applied Physics*, vol. 82, no. 12, pp. 6326–6342, Dec. 1997, doi: 10.1063/1.366523.
[41] A. Nenashev, J. Oelerich, and S. Baranovskii, "Theoretical tools for the description of charge transport in disordered organic semiconductors," *J. Phys. Condens. Matter*, vol. 27, no. 9, p. 93201, 2015, doi: 10.1088/0953-8984/27/9/093201.
[42] M. Mladenović and N. Vukmirović, "Charge Carrier Localization and Transport in Organic Semiconductors: Insights from Atomistic Multiscale Simulations," *Adv. Funct. Mater.*, vol. 25, no. 13, pp. 1915–1932, Apr. 2015, doi: 10.1002/adfm.201402435.
[43] W. L. Kalb and B. Batlogg, "Calculating the trap density of states in organic field-effect transistors from experiment: A comparison of different methods," *Phys. Rev. B*, vol. 81, no. 3, p. 035327, Jan. 2010, doi: 10.1103/PhysRevB.81.035327.
[44] S. D. Baranovskii, "Theoretical description of charge transport in disordered organic semiconductors," *physica status solidi (b)*, vol. 251, no. 3, pp. 487–525, 2014, doi: https://doi.org/10.1002/pssb.201350339.
[45] O. Simonetti, L. Giraudet, and D. Bugnot, "Effective mobility in amorphous organic transistors: Influence of the width of the density of states," *Organic Electronics*, vol. 15, no. 1, pp. 35–39, Jan. 2014, doi: 10.1016/j.orgel.2013.10.002.

[46] Y. Roichman and N. Tessler, "Generalized Einstein relation for disordered semiconductors—implications for device performance," *Appl. Phys. Lett.*, vol. 80, no. 11, pp. 1948–1950, Mar. 2002, doi: 10.1063/1.1461419.
[47] Y. Lee *et al.*, "Parametrization of the Gaussian Disorder Model to Account for the High Carrier Mobility in Disordered Organic Transistors," *Phys. Rev. Applied*, vol. 15, no. 2, p. 024021, Feb. 2021, doi: 10.1103/PhysRevApplied.15.024021.
[48] U. Wolf, H. Bässler, P. M. Borsenberger, and W. T. Gruenbaum, "Hole trapping in molecularly doped polymers," *Chemical Physics*, vol. 222, no. 2, pp. 259–267, Oct. 1997, doi: 10.1016/S0301-0104(97)00190-0.
[49] P. M. Borsenberger, W. T. Gruenbaum, U. Wolf, and H. Bässler, "Hole trapping in tri-p-tolylamine-doped poly(styrene)," *Chemical Physics*, vol. 234, no. 1, pp. 277–284, Aug. 1998, doi: 10.1016/S0301-0104(98)00115-3.
[50] I. I. Fishchuk *et al.*, "Transition from trap-controlled to trap-to-trap hopping transport in disordered organic semiconductors," *Phys. Rev. B*, vol. 73, no. 11, p. 115210, Mar. 2006, doi: 10.1103/PhysRevB.73.115210.
[51] T. P. Nguyen, C. Renaud, P. L. Rendu, and S. H. Yang, "Investigation of defects in organic semiconductors by charge based Deep Level Transient Spectroscopy (Q-DLTS)," *Phys. Status Solidi (c)*, vol. 6, no. 8, pp. 1856–1861, Aug. 2009, doi: 10.1002/pssc.200881458.
[52] S. G. J. Mathijssen *et al.*, "Dynamics of Threshold Voltage Shifts in Organic and Amorphous Silicon Field-Effect Transistors," *Adv. Mater.*, vol. 19, no. 19, pp. 2785–2789, Oct. 2007, doi: 10.1002/adma.200602798.
[53] R. Schmechel and H. von Seggern, "Electronic traps in organic transport layers," *physica status solidi (a)*, vol. 201, no. 6, pp. 1215–1235, 2004, doi: 10.1002/pssa.200404343.
[54] A. Stankevych *et al.*, "Density of States of OLED Host Materials from Thermally Stimulated Luminescence," *Phys. Rev. Applied*, vol. 15, no. 4, p. 044050, Apr. 2021, doi: 10.1103/PhysRevApplied.15.044050.

Graphical abstract